

# EXPERIENCE OF HIGH RESOLUTION VLBI IMAGING USING GENERALIZED MAXIMUM ENTROPY METHOD

A.T.BAJKOVA

*Institute of Applied Astronomy of RAS, St.Petersburg*

*(Received December 27, 2000)*

The generalized maximum entropy method (GMEM) is a special modification of the standard maximum entropy method (MEM) which seeks solutions in the space of complex functions. In this work a reduced version of the GMEM intended for reconstructing real images with positive and negative values is used. As compared with the standard MEM, intended for the reconstruction of only non-negative images, the GMEM allows us to obtain higher-quality images with a much lower level of nonlinear distortions caused by errors in the data. Here, we present the results of the GMEM imaging of 36 selected extragalactic radio sources with a resolution of 0.3-0.5 mas on astrometric and geodetic VLBI observations at 8.2 GHz, obtained with a global array in the period from 1994-1996. In VLBI mapping practice this is the first experience of imaging with such a high resolution using maximum entropy technique. A differential maximum entropy method intended for increasing the dynamic range of images is demonstrated on the radio source 0059+581. In the case of unreliable 'closure' phases, completely 'phaseless' methods of mapping are recommended. Maps of two sources 0615+820 and 0642+214 are obtained using one such method.

KEY WORDS VLBI imaging, generalized maximum entropy method, compact extragalactic radio sources

## 1 INTRODUCTION

There are two main deconvolution algorithms in Very Long Baseline Interferometry (VLBI) imaging: CLEAN and maximum entropy method (MEM). The maximum entropy method is well known among physicists as a very powerful tool for the nonlinear regularization of incorrect tasks. But in spite of its high super resolution effect, MEM is less popular in VLBI. There are two main reasons: the high computational complexity and the nonlinear image distortions caused by errors in data (visibility function). But the situation can be change fundamentally by introducing into VLBI imaging an effective modification of the MEM called the generalized maximum entropy method (GMEM) which generally operates in the space of complex functions (Bajkova, 1990, 1993). Searching for solutions of complex functions in space allows us firstly to factor multidimensional MEM algorithms into series of simpler one-dimensional algorithms, which considerably decreases the computational complexity (Frieden and Bajkova, 1994) and, secondly, considerably decreases the nonlinear distortions of images (Bajkova, 1995).

Thus, due to its generalized form MEM can become preferable in VLBI to CLEAN, especially for imaging sources with a complicated extended structure (we know, that MEM produces maximally smooth images, but CLEAN sharpens them).

In this paper we present the first experience of applying the GMEM to mapping compact extragalactic sources with high resolution (0.3-0.5 mas). We used VLBI astrometric and geodetic observations (NEOS-A program) obtained with a global array at 8.2 GHz. Data were received from the Goddard Space Flight Center. Source imaging from astrometric and geodetic VLBI observations is of great interest both for astrometry, geodesy (geodynamics taking into account extended source structure on mas scales to more accurate determination of celestial/terrestrial coordinates) and astrophysics (investigation of the short-period structure variability of compact extragalactic radio sources).

For mapping we used the well-known ‘CalTech VLBI Program’ package into which we introduced the GMEM procedure as a deconvolution operation in the selfcalibration loop.

## 2 MAPPING COMPACT EXTRAGALACTIC RADIO SOURCES

For VLBI source mapping a reduced version of the GMEM intended for the reconstruction of real signals with positive and negative values was used. The selection of the GMEM instead of the MEM as a deconvolution operation was principally dictated by low signal-to-noise ratio typical of astrometric and geodetic VLBI observations.

A detailed description of the practical GMEM algorithm is given in Bajkova (1998a). The size of maps was chosen as  $256 \times 256$  pixels, with an interval between two pixels of 0.1 mas and an image domain size between  $60 \times 60$  and  $100 \times 100$  pixels, depending in each case on structure extent and data quality. Parameter ‘ $\alpha$ ’ (Bajkova, 1990, 1998a) in the GMEM algorithm, which is responsible for separating ‘positive’ and ‘negative’ solutions, was chosen equal to  $10^8$ . A numerical solution of the entropic functional was realized using steepest-descent method. To ensure the high stability of the numerical algorithm to noise, an additional regularizing term was added to the principal entropic functional (Bajkova, 1998a).

Images of 36 selected compact extragalactic radio sources are shown in Figure 1. Characteristics of the sources are given in Table 1. Parameters of the maps (date of observations, list of VLBI stations, flux densities and agreement factors) are given in Table 2. The presented images were obtained by convolution of entropic solutions by a circular gaussian beam with a circle diameter on 0.2 mas. This size is enough to smooth over image samples distant which are 0.1 mas from each other (the beam circles are shown in bottom left corner of the maps).

The GMEM images can be compared with the corresponding CLEAN images published in Bajkova *et al.* (1996a). The comparison shows, that the GMEM maps are obtained with better agreement factors (nearly in 2.2 times) and are less ‘lumpy’. In this connection the total flux increased on the average by 1.036 times, i.e. practically did not change. But the peak flux decreased by 1.83 times. Taking into account this and the fact that MEM and GMEM principally seek a solution in space of smooth gaussian functions, it is possible to conclude that the new GMEM maps are smoother than the CLEAN maps.

**Table 1.** List of sources

<i>Source</i>	<i>Alias</i>	<i>Ident.</i>	<i>z</i>	<i>m<sub>v</sub></i>	<i>S<sub>6</sub></i>	<i>S<sub>3.5</sub></i>
0014+813	S5 0014+81	QSO	3.384	16.50	0.551	1.355
0016+731	S5 0016+73	QSO	1.781	18.00	1.700	1.900
0059+581	-	-	-	-	-	2.800
0202+149	4C +15.05, NRAO 91	QSO	-	21.90	2.400	3.100
0229+131	4C +13.14	QSO	2.067	17.03	1.000	1.900
0336-019	CTA 26	QSO	0.852	18.41	2.500	2.800
0400+258	-	QSO	2.109	18.00	1.800	1.400
0402-362	-	QSO	1.417	17.17	1.400	-
0440+345	-	-	-	-	-	-
0458-020	4C -02.19	QSO	2.286	19.50	1.900	3.100
0528+134	-	QSO	2.070	20.30	3.900	4.500
0552+598	DA 193	QSO	2.365	18.00	5.400	5.700
0615+820	-	QSO	0.710	17.50	0.999	0.900
0642+214	3C 166, 4C +21.21	G	0.245	19.50	1.100	-
0716+714	-	LAC	-	15.50	1.121	0.600
0735+178	OI 158	LAC	0.424	16.22	1.800	1.900
0917+624	OK 630	QSO	1.446	19.50	0.996	1.500
0955+476	OK 492	QSO	1.873	18.00	0.739	0.700
1014+615	-	BSO	-	18.10	0.631	0.571
1101+384	Mkn 421	G	0.031	13.10	0.725	0.700
1128+385	OM 346.9	QSO	1.733	16.00	0.771	0.900
1219+285	W Com, ON 231	LAC	0.102	16.11	2.000	0.700
1308+326	AU CVn	LAC	0.996	19.00	1.500	3.700
1357+769	-	QSO	-	19.00	0.844	0.600
1606+106	4C +10.45	QSO	1.226	18.50	1.400	1.600
1637+574	OS 562	QSO	0.751	17.00	1.400	1.700
1638+398	NRAO 512	QSO	1.666	16.50	1.160	1.500
1739+522	4C +51.37, OT 566	QSO	1.375	18.50	2.000	1.200
1741-038	-	QSO	1.057	18.60	3.000	3.000
1745+624	4C +62.29	QSO	3.886	18.70	0.580	0.480
1803+784	-	LAC	0.684	16.40	2.600	2.400
1823+568	4C +56.27	LAC	0.664	18.40	1.700	2.100
2145+067	4C +06.69	QSO	0.990	16.47	4.500	8.600
2200+420	BL Lac, VRO 42.22.01	LAC	0.068	14.72	4.800	5.900
2201+315	4C +31.63	QSO	0.297	15.79	2.300	2.500
2230+114	CTA 102, 4C +11.69	QSO	1.037	17.66	3.600	3.600

Improvement of agreement factors in case of GMEM shows that the space of smooth functions for searching for source distributions is more adequate than the space of  $\delta$ - functions in which the CLEAN solutions are sought, i.e. the considered sources reveal rather extended structure at the given resolution. Note that CLEAN always gives disconnected solution as a combination of  $\delta$ - functions (in addition, CLEAN sharpens bright components and damps weak ones), although CLEAN maps usually seem smooth. This is because a CLEAN map is a convolution of the CLEAN solution (model) by a smooth gaussian ‘clean’ beam. And, obviously, in general a CLEAN map is not obliged to agree with the data to such an extent as the corresponding CLEAN model. But when we use the GMEM we at once obtain a smooth solution which is in good agreement with the data.

**Table 2.** Parameters of maps

<i>Source</i>	<i>Date</i>	<i>Stations</i>	<i>Flux</i> <i>total</i>	<i>[Jy]</i> <i>peak</i>	<i>Agr.</i> <i>ampl.</i>	<i>factor</i> <i>phase</i>	<i>total</i>
0014+813	17.10.95	G,W,N20,MK,NL,A,K	0.960	0.234	2.32	2.79	2.52
0016+731	18.01.94	F,W,G,K,MK,SC,N85	1.760	0.244	1.81	1.66	1.75
0059+581	27.06.95	G,W,NY,F,N85,	1.620	0.825	1.77	1.20	1.61
0202+149	09.01.96	NY,W,F,N20,G,K	1.310	0.592	3.15	1.59	2.77
0229+131	18.01.94	F,W,G,SC,N85,BR,K,MK	1.430	0.318	1.65	1.66	1.65
0336-019	18.01.94	F,W,SC,N85,BR,K,G,MK	2.070	0.737	2.02	1.92	1.99
0400+258	09.01.96	F,W,NY,N85,G,K	0.320	0.131	0.81	0.84	0.82
0402-362	23.01.95	F,H26,MA,H,S,N85,SS,MK,P	1.260	0.935	1.51	1.21	1.39
0440+345	22.08.95	K,NY,G,W,F,N85	0.430	0.131	1.41	1.95	1.61
0458-020	23.01.95	F,MA,H,N85,SC,P, S,MK,H26,C	1.500	0.693	2.18	1.62	2.00
0528+134	01.02.95	C,D65,MA,ME,NY,W,O,N	3.840	1.317	3.94	1.45	3.12
0552+398	04.01.94	F,N85,K,W,G,A	3.840	1.212	2.26	1.11	1.98
0615+820	26.03.96	G,K,W,NY,N20	0.300	0.079	1.33	–	–
0642+214	14.11.95	G,K,NY,W,F,N85	0.380	0.152	1.78	–	–
0716+714	14.11.95	NY,W,G,K,F,N85	0.180	0.111	0.96	1.15	1.02
0735+178	18.01.94	F,W,SC,G,BR,K,MK	1.540	0.299	2.59	2.84	2.68
0917+624	05.03.96	NY,W,N20,F,G,K	1.090	0.222	1.81	1.37	1.67
0955+476	18.01.94	G,K,W,BR,F,SC,MK	0.970	0.393	1.38	1.52	1.45
1014+615	06.02.96	G,K,N20,W,F	0.340	0.136	1.87	2.01	1.92
1101+384	17.10.95	A,G,NL,MK,K,W	0.350	0.124	1.43	2.87	1.14
1128+385	31.10.95	G,NY,K,N85,W,F	0.630	0.268	1.31	1.37	1.33
1219+285	31.10.95	G,NY,K,N85,W,F	0.210	0.067	0.99	1.00	0.99
1308+326	04.10.94	G,K,MK,W,F,SC,BR	3.490	1.249	3.46	2.96	3.32
1357+769	17.10.95	A,G,N20,W,NL,MK,K,F	0.590	0.276	1.52	2.49	1.96
1606+106	18.01.94	G,N85,K,BR,MK,F,W,SC	1.310	0.420	1.23	1.98	1.51
1637+574	05.03.93	K,N20,G,NY,W,F	0.850	0.322	2.15	1.17	1.87
1638+398	08.08.95	N85,W,G,K,F	0.630	0.276	1.01	1.76	1.29
1739+522	18.01.94	K,W,BR,MK,SC,N85,F	1.080	0.267	1.66	1.80	1.71
1741-038	18.01.94	G,K,BR,MK,N85,SC,F,W	2.830	0.898	1.67	2.75	2.07
1745+624	03.10.95	G,K,W,N20,F	0.200	0.109	0.61	0.71	0.64
1803+784	18.01.94	BR,MK,G,N85,K,SC,W,F	1.710	0.575	3.53	3.81	3.64
1823+568	03.10.95	G,W,N20,F,K	0.600	0.324	3.76	2.32	3.32
2145+067	17.10.95	A,F,G,N20,W,NL,MK,K	8.010	1.838	6.37	10.0	7.88
2200+420	26.03.96	G,K,W,NY,N20,F	2.810	0.491	4.38	2.88	3.97
2201+315	18.01.94	F,W,BR,MK,SC,N85,G,K	1.950	0.306	1.59	2.56	1.99
2230+114	31.10.95	NY,W,F,N85,G,K	1.070	0.295	1.78	1.08	1.66

Abbreviations: **A** – Algotpark; **BR** – VLBA-BR; **C** – Crimea; **D65** – DSS65; **F** – Fortleza; **G** – Gilcreek; **H** – Hartrao; **H26** – Hobart26; **K** – Kokee; **MA** – Matera; **ME** – Medicina; **MK** – VLBA-MK; **N** – Noto; **N20** – NRAO20; **N85** – NRAO85; **NL** – VLBA-NL; **NY** – NyAlesund20; **O** – Onsala; **SC** – VLBA-SC; **W** – Wettzell.

If we obtain GMEM solution with a worse agreement factor than the CLEAN one, we should conclude that in this case GMEM is less adequate than CLEAN and the source can be considered to be point-like source consisting of some  $\delta$ - functions. In our case, such a source is 0642+214 (in fact, its CLEAN solution has better agreement factor than the GMEM solution (by approximately two times)).

On the basis of careful analysis of both the CLEAN and GMEM maps we can conclude that the GMEM gave more accurate estimates of source distributions than the CLEAN map. In some of the sources (0400+258, 0458-020, 0917+624, 1606+106, 1823+568, 2230+114) the extended structure details are revealed to a fuller extent. All the images are free from the artifacts inherent in CLEAN.

To increase the dynamic range of the maps we used a differential GMEM (see Section 3). A more detailed comparison of CLEAN and GMEM images is given in Bajkova (1999).

It is also necessary to note that the maps of two sources with unreliable ‘closure’ phases 0615+820 and 0642+214 were obtained using completely ‘phaseless’ mapping (see section 4).

### 3 A DIFFERENTIAL METHOD OF MAXIMUM ENTROPY

At present, the idea of differential mapping is realized most comprehensively in the ‘DIFMAP’ program package at the CalTech, where CLEAN method is used as the deconvolution operation.

The method of differential mapping is based on the fundamental linear property of linearity of the Fourier transformation. According to this method, the bright components of the source, which were reconstructed at the first stage, are subtracted from the initial visibility function, the subsequent reconstruction is performed using the residual visibility function, and the reconstruction results are added at the final stage.

In the case of CLEAN, such a mapping method mainly influences the convergence rate. However, if the MEM, which has pronounced nonlinear properties, is used as the deconvolution operation, the principle of differential mapping can improve the reconstruction quality, particularly when the source has bright compact components against the background of a sufficiently weak extended base.

What is the cause of the reconstruction quality improvement? The fact is that after the subtraction of bright components, which were reconstructed at the first stage using the MEM, from the initial visibility function we obtain the residual visibility function, in which the proportion of the weak extended component becomes larger. Therefore, we artificially decrease the dynamic interval of the map, which corresponds to the residual visibility function, thus simplify the image reconstruction at the second stage.

Above we discussed the advantages of the GMEM for processing real non-negative images. With respect to differential mapping, another advantage of GMEM originated from the fact that an image with negative values can correspond to the residual visibility function after subtraction of the bright component that is reconstructed at the first stage of the algorithm from the initial visibility function. This is possible if the bright component was reconstructed at the first stage with an overestimated amplitude, which is quite typical of any nonlinear method. To rule out unwanted image distortions when a non-negative solution is sought using the data assuming the presence of negative components, we should use the generalized method rather than the standard one.

Simulation results of the differential GMEM are shown in Bajkova (1998b). Here we demonstrate potential of differential GMEM for mapping the radio source 0059+581, which is actively used as a reference source in the astrometric and geodetic VLBI programs. This source is of interest because it shows fast variation of both the total flux and the structure, which consists of a compact core and rather weak extended elements (jet). The maps that were constructed using GMEM for a number of dates between June 1994 and December 1995 are shown in Bajkova (1998b). Between the middle and the end of 1994 we observed an almost linear decrease in the

total flux from  $\sim 4$  Jy to 1.5 Jy. As is obvious from Bajkova (1998b), we failed to obtain a map with a sufficient dynamic range to detect an extended element from June 26, 1994, when the flux was maximal over the interval in question. Using the standard GMEM, we only detected extended elements from October 4, 1994, when their share with respect to the total flux became sufficient to be detected by the selected reconstruction method. In Figure 2, for comparison, we show maps, obtained using both the standard and differential GMEM for three dates on which the total flux was sufficiently large and the flux share corresponding to extended elements was insignificant. As is obvious from the figure, the use of differential mapping allowed us to increase the dynamic range of the maps such that the extended structures became very distinguished.

#### 4 ‘PHASELESS’ MAPPING

A principle of ‘phaseless’ mapping used for imaging two sources 0615+820 and 0642+214 (see Figure 1) is based on reconstruction of the visibility function amplitude over the whole  $UV$ -plane. The image is then reconstructed using only the amplitude of the visibility function (the well-known ‘phase problem’). For reconstruction of the visibility amplitude GMEM has also been used in the self-calibration loop setting all the ‘closure’ phases to zero. For solving the ‘phase problem’ an effective modification of the well-known Fienup algorithm was used (Bajkova, 1996b). ‘Phaseless’ mapping is recommended in the case of bad ‘closure’ phases.

#### 5 SUMMARY

This work is devoted to the first experience of the high resolution imaging of compact extragalactic sources using generalized maximum entropy method proposed by the author in earlier papers (Bajkova, 1990, 1993). Images of a sample of 36 selected compact extragalactic radio sources obtained with a resolution of 0.3–0.5 mas on astrometric and geodetic VLBI observations at 8.2 GHz with a global array (NEOS-A program) between 1994 and 1996 are presented. Comparison with the corresponding CLEAN images shows that the images obtained are smoother and characterized by better agreement factors, revealing rather complicated structures to a fuller extent.

The choice of reconstruction method as the deconvolution procedure in self-calibration loop depends on the signal-to-noise ratio and *a priori* information about the source’s structure. In the case of point-like structures, which are the majority of sources observed in geodetic programs, the traditional CLEAN is the preferable procedure because it was invented especially for such sources and is very fast. In the case of complicated structures with strongly extended components, the nonlinear information methods can be preferable. Moreover, in the case of a low signal-to-noise ratio, which is typical for astrometric and geodetic VLBI observations, the generalized information methods for seeking a solution in the space of functions with positive and negative values are preferable to the standard ones which deal only with real non-negative distributions, because they ensure a much lower level of nonlinear distortions.

To increase the dynamic range of images we used a differential generalized maximum entropy method. Compared with the traditional methods, the nonlinear methods of differential mapping using the maximum entropy method as the deconvolution operation allow us to substantially

improve the reconstruction quality of source images containing bright point components against a background of a weak base. The maps obtained using the differential method of maximum entropy are characterized by a higher dynamic range. To eliminate possible nonlinear distortions in the case of differential mapping, the generalized method of maximum entropy is preferred to the standard method.

In the case of unreliable ‘closure’ phases we recommend using completely ‘phaseless’ methods of mapping.

#### *Acknowledgments*

This work was supported by Federal Program ‘Astronomy’ (Grant No 2.1.1.3.).

#### *References*

- Bajkova, A.T. (1990) *Astron. Astrophys. Trans.* **1**, 313.
- Bajkova, A.T. (1993) *Maximum Entropy and Bayesian Methods*. Kluwer Academic, 407.
- Bajkova, A.T. (1995) *Izvestia vuzov. Radiofizika.* **38**, 1267 (in Russian).
- Bajkova A.T. et al. (1996a) *Communications of IAA RAS*, **87**, St.Petersburg (in Russian).
- Bajkova, A.T. (1996b) *Izvestia vuzov. Radiofizika.* **39**, 472 (in Russian).
- Bajkova, A.T. (1998a) *Trudy IPA RAN.* **3**, 287 (in Russian).
- Bajkova, A.T. (1998b) *Izvestia vuzov. Radiofizika.* **41**, 991 (in Russian).
- Bajkova, A.T. (1999) *Trudy IPA RAN.* **4**, 150 (in Russian).
- Frieden, B.R., Bajkova, A.T. (1994) *Applied Optics*, **33**, 219.

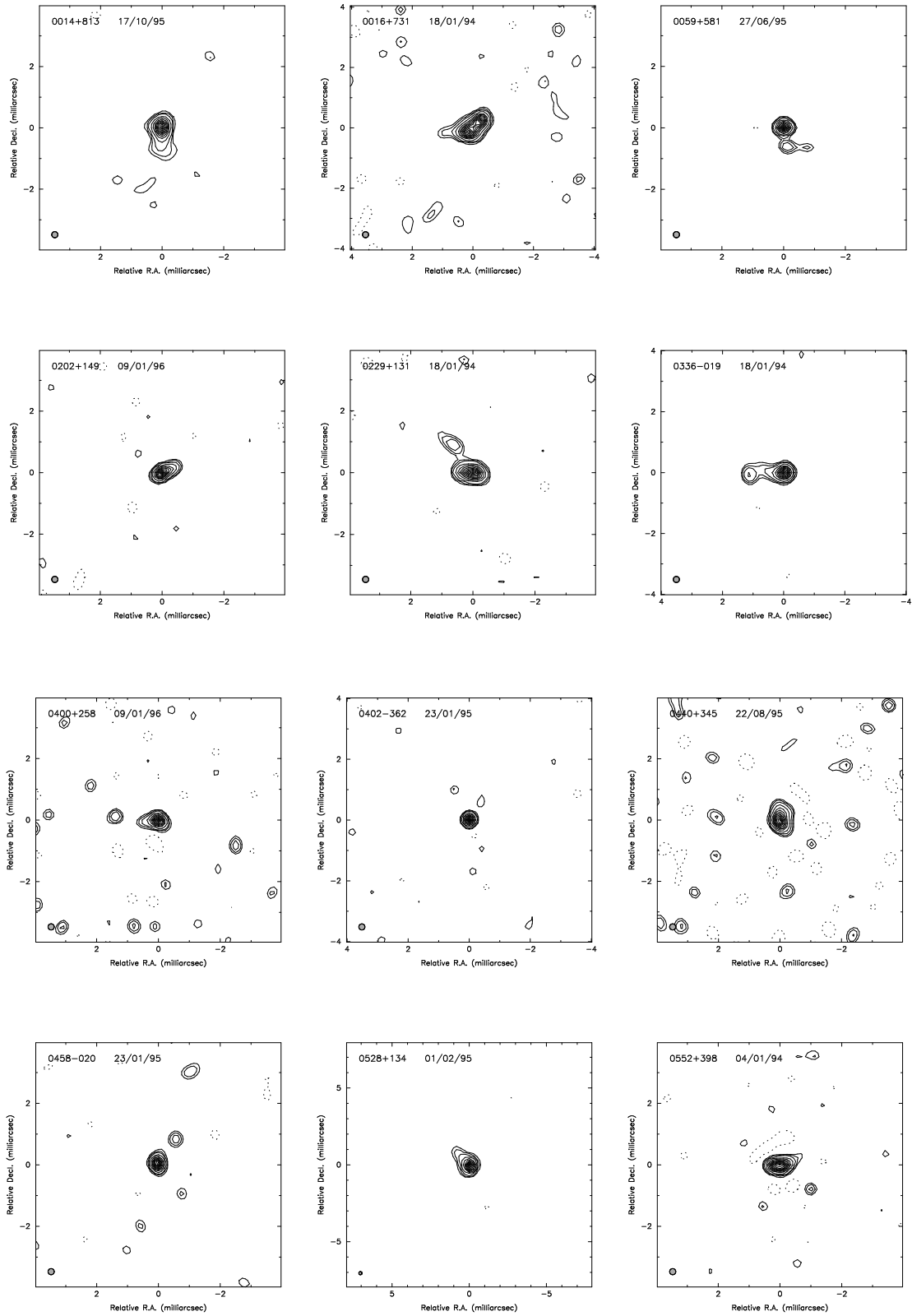


**Figure 1** Images of extragalactic sources obtained by GMEM. Contour levels are 1, 2, 4, 10, 20, 30, 40, 50, 60, 70, 80, 90, 99 % of peak intensity.



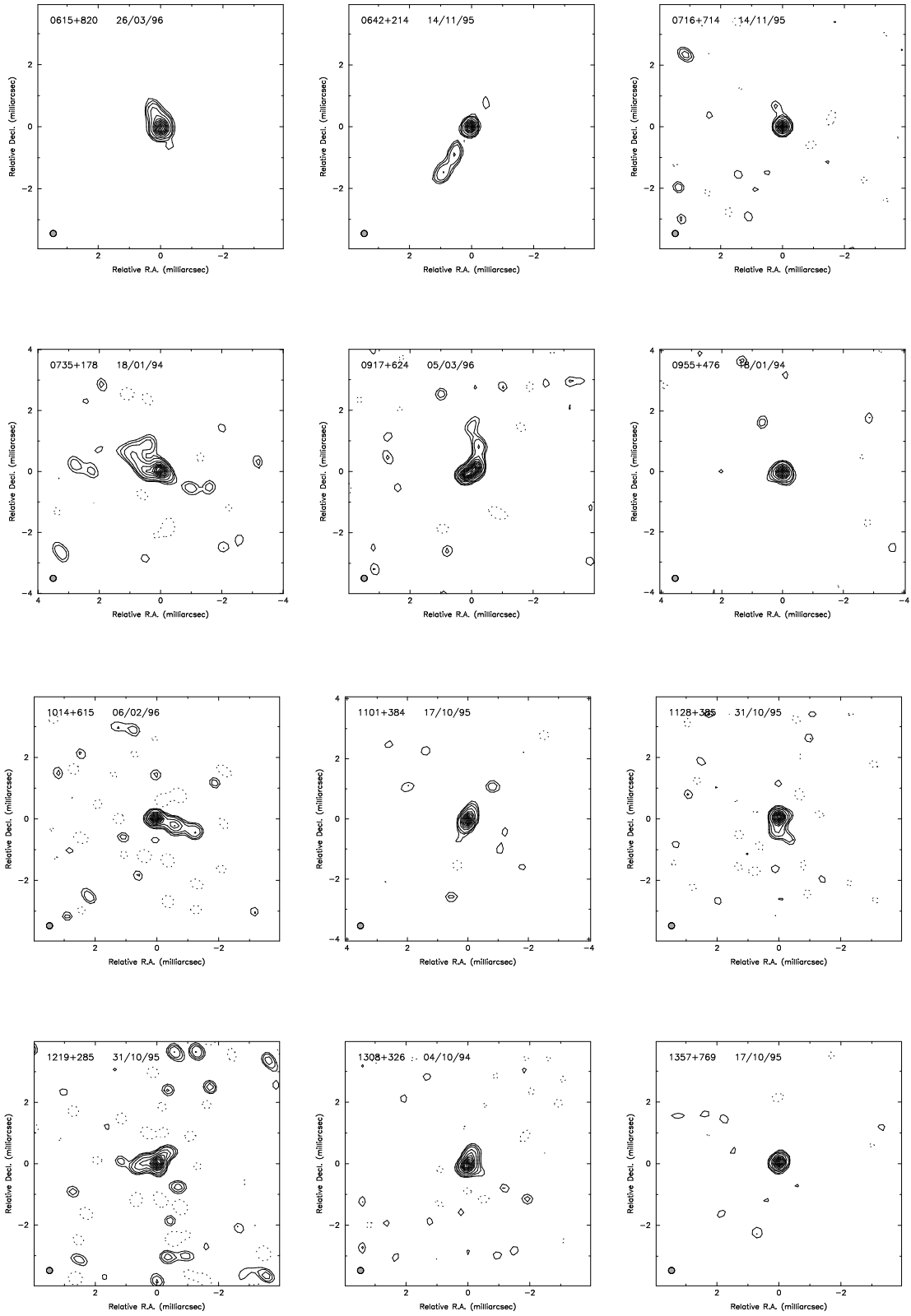


Figure 1 (Continued).

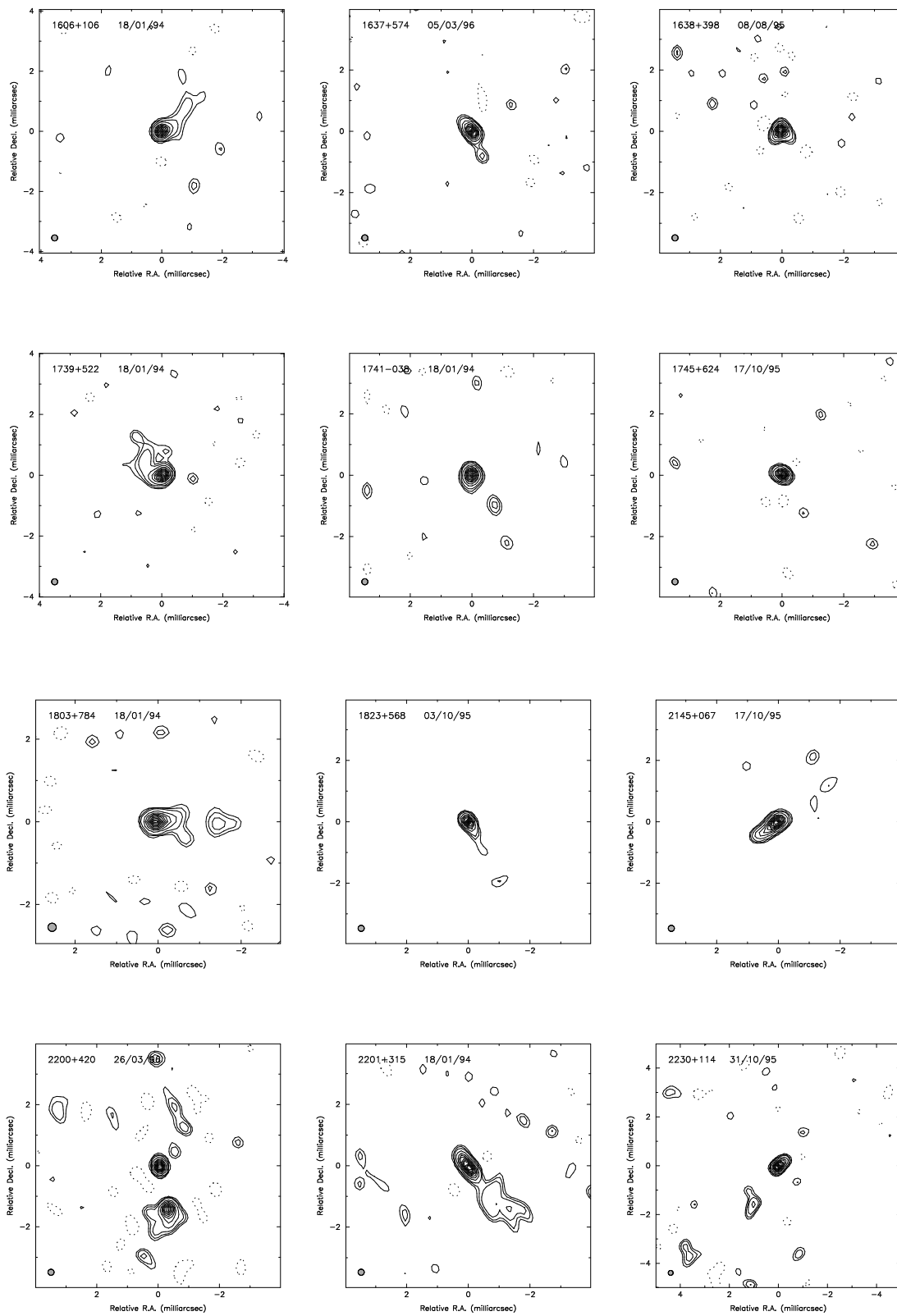
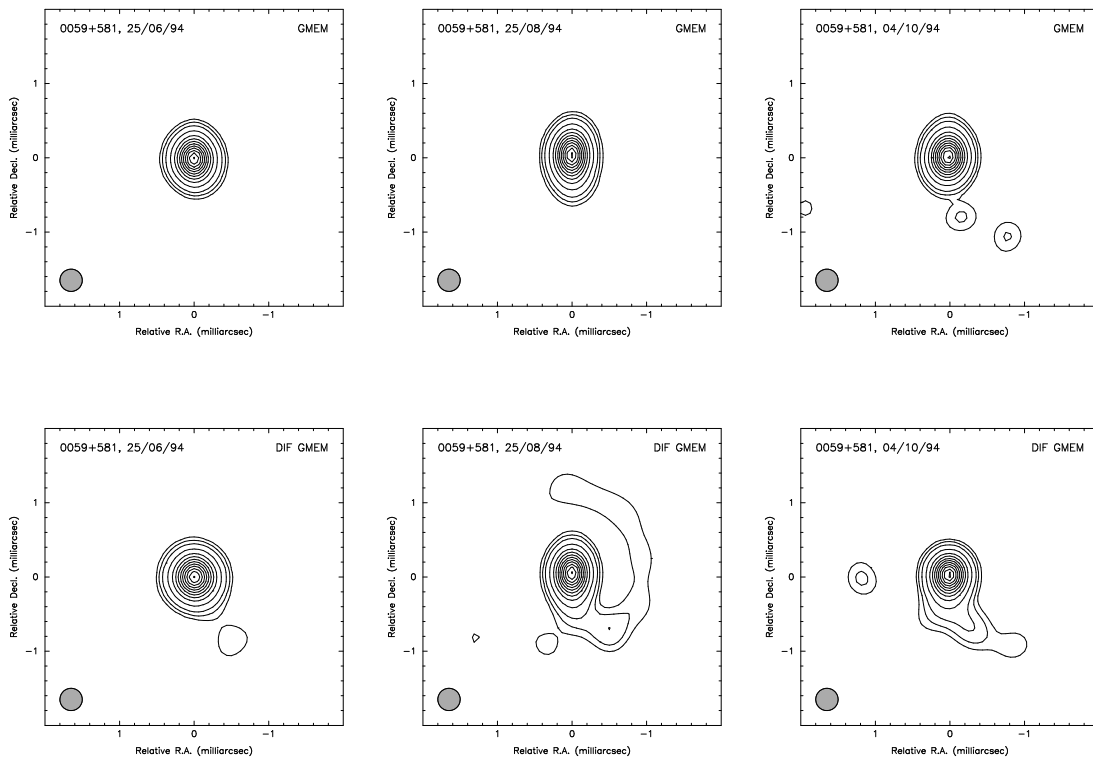


Figure 1 (Continued).



**Figure 2** Images of source 0059+581 obtained by the standard GMEM (top) and the differential GMEM (bottom) for three dates. Contour levels are 1, 2, 4, 10, 20, 30, 40, 50, 60, 70, 80, 90, 99 % of peak intensity.